IEEE Access
Multidisciplinary | Rapid Review | Open Access Journal

Received July 12, 2019, accepted August 16, 2019, date of publication September 3, 2019, date of current version September 25, 2019.

Digital Object Identifier 10.1109/ACCESS.2019.2939258

LS-SVM Inverse System Decoupling Control Strategy of a Bearingless Induction Motor Considering Stator Current Dynamics

WENSHAO BU[1,2] AND ZIYUAN LI[1]

[1]Electrical Engineering College, Henan University of Science and Technology, Luoyang 471023, China
[2]Information Engineering College, Henan University of Science and Technology, Luoyang 471023, China

Corresponding author: Wenshao Bu (wsbu@163.com)

This work was supported by the National Natural Science Foundation of China under Grant 51277053.

ABSTRACT The bearingless induction motor (BL-IM) is a multivariable, nonlinear and strongly coupled object, in order to achieve its dynamic decoupling control with high performance, on the basis of the least square support vector machine(LS-SVM) principle, a novel LS-SVM inverse system decoupling control strategy is proposed. Firstly, under the conditions of taking the stator current dynamics of torque windings into account, the state equations of the BL-IM system are established. Secondly, based on the approximation and identification fitting ability of the LS-SVM to arbitrary nonlinear function, the inverse system mathematical model of the BL-IM system considering the stator current dynamics is trained and obtained. After that, according to the decoupling principle of inverse system, the BL-IM system is decoupled into four second-order pseudo-linear integral subsystems, include a motor speed subsystem, a rotor flux-linkage subsystem and two radial displacement component subsystems. At the end, the comprehensive simulation analysis of the LS-SVM inverse decoupling control system are carried out. From the simulation results, it can be known that the dynamic decoupling control among the motor speed, rotor flux-linkage and two radial displacement components can be realized, meanwhile after considering the dynamics of the stator current, the LS-SVM inverse decoupling control system of BL-IM has the characteristics of fast response and strong anti-interference ability.

INDEX TERMS Bearingless induction motor system, dynamics of stator current, LS-SVM, inverse system decoupling.

I. INTRODUCTION

The AC motor supported by magnetic bearing has been widely used in the high speed drive field [1]–[4], but it still has some disadvantages, such as the higher magnetic suspension power consumption, the difficulty to over speed, etc. [5]–[8]. The bearingless motor is a new type of AC motor that is proposed based on the similarity of stator structure between ordinary AC motor and magnetic bearing [9], [10]. Normally, there are two sets of windings in the stator slots of bearingless motor, one is the torque windings with current angular frequency ω_1 and pole-pair number p_1, another is the suspension windings with current angular frequency ω_2 and pole-pair number p_2 [5], [10]. The magnetic field produced by the torque windings, i.e. the so-called motor magnetic field, is used for the rotary drive of bearingless rotor, while the suspension control magnetic field produced by the suspension windings breaks the balance and symmetry of the motor magnetic field, and results in the magnetic field enhancement in some air-gap area, and the magnetic field weakening in the symmetrical air-gap area in space [5], [10]. When the pole-pair numbers of two sets of stator windings and their current angular frequencies meet the "$p_2 = p_1 \pm 1$, $\omega_2 = \omega_1$" conditions [5], [11]–[13], a stable resultant force in radial direction can be generated that is controllable both in amplitude and in direction, and then the suspension motion of the bearingless rotor can be freely controlled. The controllable resultant force in radial direction is called controllable magnetic suspension force. The generation principle of the controllable magnetic suspension force is shown

The associate editor coordinating the review of this manuscript and approving it for publication was Wei E.I. Sha.

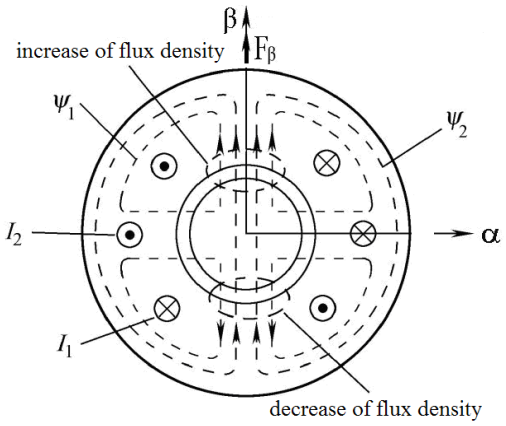

FIGURE 1. Suspension force generation schematic diagram.

in Figure 1 [10], where the pole-pair numbers p_1 and p_2 equal to 2 and 1 respectively.

Compared with the AC motor that is supported by magnetic bearings, the shaft of the bearingless motor is shorter, the critical speed of the bearingless rotor is higher, and then the bearingless motor is more suitable for the high-speed rotary drive application [5], [10], [15]–[17]. Now, in aerospace, advanced manufacturing, semiconductor processing, chemical industry, life sciences and biopharmaceutical fields, an urgent requirement has been proposed for the bearingless motor technology. The bearingless motor technology can be applied to various AC motors, and among them, because of a series of advantages, such as a robust structure, a larger force/current ratio and the convenience for weakening magnetic, the bearingless induction motor (BL-IM) has attracted wide attention [18]–[23].

Inside the BL-IM, there exists complex electromagnetic coupling relationship [18]–[20]. In order to achieve its dynamic control with high performance, the dynamic decoupling among relevant controlled variables should be achieved [21], [22]. The inverse system method is an effective linearization method based on nonlinear feedback [22]–[24], its physical concepts is clear and intuitive, and it can be used for the dynamic decoupling of all kinds of bearingless motors.

In the analytical inverse system method, the derived analytical inverse system model of the controlled object is always very complicated; meanwhile, the model accuracy is unavoidably affected by the modeling deviation and time-varying parameters, this will inevitably affect the decoupling performance of the BL-IM system [10], [22], and then it is inconvenient for practical application. Utilizing the neural network, the nonlinear inverse model of a BL-IM system can be identified [21], [22]. But the problems of neural network itself, such as the slower convergence rate, the easiness to fall into local minima and the more dependence on the expert knowledge, have limitited its application scope to a certain extent [25]. The support vector machine (SVM) is a novel machine learning method that is based on the statistical learning theory [26], it can effectively minimize the dependence on the expert knowledge. In addition, the SVM also has some other excellent characteristics, such as the small sample self-learning ability, the stronger generalization ability, the global optimization ability and the relatively fixed topological structure, etc. [25], and then it is very suitable for the parameter estimation and model identification. The least squares support vector machine (LS-SVM) is a further expansion of the SVM [25], [27], it changes the inequality constraint of traditional SVM to an equivalent equality constraint, it converts the problem of solving the quadratic programming to that of solving linearization equations [25], it effectively simplifies the computation process [6], [25], [28], and then it is applicable to the nonlinear modeling of the bearingless motor system [25], [28]. About the decoupling control strategies of BL-IM system based on the LS-SVM, there have been some research processes. But in the existing researches [29]–[31], the stator current components are selected as the control inputs of the original system, therefore the dynamics of stator current are not taken into account, and as a result, the identified inverse model of the BL-IM system is not accurate enough [28]–[31], which inevitably limits the improvement of the dynamic decoupling control performance of the BL-IM system to a certain extent.

In order to control the BL-IM with high-performance, this paper proposes a LS-SVM inverse decoupling control strategy for the BL-IM system. Firstly, taking the current dynamic link of torque windings into account, and on the basis of the rotor flux-linkage orientation of the torque system, the state equations of a BL-IM system are established firstly [22]. And then, on the basis of the reversibility analysis, the LS-LVM inverse system model of a BL-IM system is trained and established, by way of the inverse system method, the BL-IM system is decoupled into four second-order pseudo-linear integral subsystems [22], meanwhile the analysis and synthesis are made for each subsystem. At the end, the proposed LS-SVM inverse decoupling control strategy is simulated and verified in detail.

II. MATHEMATICAL MODEL OF A BL-IM SYSTEM

A. MATHEMATICAL MODEL OF THE TORQUE SYSTEM

During the normal operation of a BL-IM system, because the rotor's eccentricity is very small, the influence of the suspension control magnetic field on the torque windings can be neglected. And then, the mathematical model of torque system is basically the same as that of the ordinary induction motor system.

Defining d-q is the coordinate system oriented by the rotor flux-linkage of torque system [22], [24]. Then, considering the dynamic differential equations of the stator current components, and taking the constraint conditions "$\psi_{r1q} = \dot{\psi}_{r1q} = 0$, $\psi_{r1} = \psi_{r1d}$" into account, the dynamic mathematical model of the torque system can be obtained

as follows [24]:

$$\begin{cases} \dfrac{di_{s1d}}{dt} = -\dfrac{R_{s1}L_{r1}^2 + R_{r1}L_{m1}^2}{\sigma L_{s1}L_{r1}^2} i_{s1d} + \omega_1 i_{s1q} \\ \qquad + \dfrac{L_{m1}}{\sigma L_{s1}L_{r1}T_{r1}}\psi_{r1} + \dfrac{1}{\sigma L_{s1}} u_{s1d} \\ \dfrac{di_{s1q}}{dt} = -\dfrac{R_{s1}L_{r1}^2 + R_{r1}L_{m1}^2}{\sigma L_{s1}L_{r1}^2} i_{s1q} - \omega_1 i_{s1d} \\ \qquad - \dfrac{L_{m1}}{\sigma L_{s1}L_{r1}}\omega\psi_{r1} + \dfrac{1}{\sigma L_{s1}} u_{s1q} \\ \dfrac{d\psi_{r1}}{dt} = -\dfrac{1}{T_{r1}}\psi_{r1} + \dfrac{L_{m1}}{T_{r1}} i_{s1d} \\ \dfrac{d\omega_r}{dt} = \dfrac{p_1 L_{m1}}{JL_{r1}}\psi_{r1} i_{s1q} - \dfrac{1}{J} T_L \end{cases} \tag{1}$$

where, the expression of the synchronous angular speed ω_1 is as follow:

$$\omega_1 = p_1\omega_r + \frac{L_{m1} i_{s1q}}{T_{r1}\psi_{r1}} \tag{2}$$

In (1) and (2): ψ, u, i, R represent the flux-linkage, voltage, current and resistance respectively; the subscripts s1 and $r1$ represent the stator and rotor of torque system respectively; ω_r is the rotation angular velocity of the bearingless rotor; the subscripts d and q represent the corresponding components in d-q coordinate system; L_{r1}, L_{s1} and L_{m1} represent the rotor self-inductance, the stator self-inductance and the mutual inductance respectively; L_{s1l} and L_{r1l} are the stator- and rotor-leakage inductance respectively; T_L is the load torque variable; T_{r1} is the time constant of rotor windings.

B. MATHEMATICAL MODEL OF MAGNETIC SUSPENSION SYSTEM

Defining α-β is the stationary coordinate system whose coordinate origin is set on the stator axis. Then the components of controllable magnetic suspension force in the α-β coordinate system can be expressed as follows [24]:

$$\begin{cases} F_\alpha = K_m(i_{s2d}\psi_{1d} + i_{s2q}\psi_{1q}) \\ F_\beta = K_m(i_{s2d}\psi_{1q} - i_{s2q}\psi_{1d}) \end{cases} \tag{3}$$

where, K_m is the stiffness coefficient of magnetic suspension force that is determined by the BL-IM structure; the expression of coefficient K_m is as follow:

$$K_m = \pi L_{m2}/(4\mu_0 lrN_1N_2) \tag{4}$$

In (3) and (4): F_α and F_β are the components of controllable magnetic suspension force in the α-β coordinate system [24], [25]; i_{s2d} and i_{s2q} are the components of magnetic suspension control current in the d-$q$coordinate system; μ_0 is the air-gap permeability; l is the length of stator core; r is the inner diameter of stator core; L_{m2} is the excitation inductance per phase of the three-phase suspension windings; N_1 is the effective turn number in series per phase of the three-phase concentrated torque windings, and N_2 is that of the three-phase concentrated suspension windings [22]; ψ_{1d} and ψ_{1q} are the air-gap flux-linkage components of the torque system in the d-q coordinate system [24], [25].

From (3), it can be known that the components of controllable magnetic suspension force is related to the components ψ_{1d} and ψ_{1q} of the air-gap flux-linkage. The required ψ_{1d} and ψ_{1q} components can be expressed as follows:

$$\psi_{1d} = \frac{L_{m1}}{L_{r1}}(\psi_{r1} + L_{r1l} i_{s1d}), \quad \psi_{1q} = \frac{L_{m1}}{L_{r1}} L_{r1l} i_{s1q} \tag{5}$$

From the principle of mechanical dynamics, the suspension motion equation of bearingless rotor can be expressed as follow [22]:

$$m\ddot{\alpha} = F_\alpha + f_\alpha + F_{L\alpha}, \quad m\ddot{\beta} = F_\beta + f_\beta + f_{L\beta} \tag{6}$$

In (6): m is the mass of bearingless rotor; in the α-β coordinate system, $F_{L\alpha}$ and $F_{L\beta}$ are the corresponding components of external radial force, f_α and f_β are the corresponding components of unilateral electromagnetic pull. Here, the expressions of f_α and f_β components are as follows:

$$f_\alpha = k_s\alpha, \quad f_\beta = k_s\beta \tag{7}$$

where, k_s is the stiffness coefficient of radial displacement [22], its expression is "$k_s = \pi rlB^2/2\mu_0\delta_0$", δ_0 is the average length of air-gap, B is the amplitude of air-gap flux density of the torque system.

C. STATE EQUATION OF A BL-IM SYSTEM

Taking the current dynamics of the torque system into account, the input-, state- and output-variable of the BL-IM system are defined as follows:

$$u = (u_1, u_2, u_3, u_4)^T = (u_{s1d}, u_{s1q}, i_{s2d}, i_{s2q})^T \tag{8}$$

$$\begin{aligned} x &= (x_1, x_2, x_3, x_4, x_5, x_6, x_7, x_8)^T \\ &= (\alpha, \beta, \dot{\alpha}, \dot{\beta}, i_{s1d}, i_{s1q}, \psi_{r1}, \omega_r)^T \end{aligned} \tag{9}$$

$$y = (y_1, y_2, y_3, y_4)^T = (\alpha, \beta, \psi_{r1}, \omega_r)^T \tag{10}$$

After substituting equations (8) $\sim$ (10) into equations (1) $\sim$ (6), an eight-order state equation of the BL-IM system can be obtained, as shown in equation (11).

$$\begin{cases} \dot{x}_1 = x_3 \\ \dot{x}_2 = x_4 \\ \dot{x}_3 = \dfrac{K_m}{m} \cdot \dfrac{L_{m1}}{L_{r1}}[(x_7 + L_{r1l}x_5)u_3 + L_{r1l}x_6u_4] + (k_sx_1 \\ \qquad +F_{L\alpha})/m \\ \dot{x}_4 = \dfrac{K_m}{m} \cdot \dfrac{L_{m1}}{L_{r1}}[L_{r1l}x_6u_3 - (x_7 + L_{r1l}x_5)u_4] \\ \qquad +(k_sx_2 + F_{L\beta})/m \\ \dot{x}_5 = -(\gamma - \delta)x_5 + (p_1x_8 + L_{m1}\delta x_6/x_7)x_6 \\ \qquad +\xi\delta\eta x_7 + \xi u_3 \\ \dot{x}_6 = -(\gamma - \delta)x_6 - (p_1x_8 + L_{m1}\delta x_6/x_7)x_5 \\ \qquad -\xi\eta x_7 p_1 x_8 + \xi u_4 \\ \dot{x}_7 = L_{m1}\delta x_5 - \delta x_7 \\ \dot{x}_8 = \mu x_6 x_7 - T_L/J \end{cases} \tag{11}$$

In (11), the related parameters are expressed as follows:

$$\gamma = \frac{R_{s1}}{\sigma L_{s1}} + \frac{R_{r1}}{\sigma L_{r1}}, \quad \sigma = 1 - \frac{L_{m1}^2}{L_{s1}L_{r1}}, \quad \delta = \frac{R_{r1}}{L_{r1}},$$
$$\xi = \frac{1}{\sigma L_{s1}}, \quad \mu = \frac{p_1 L_{m1}}{J L_{r1}}, \quad \eta = \frac{L_{m1}}{L_{r1}}.$$

III. REVERSIBILITY ANALYSIS OF THE BL-IM SYSTEM

The invertibility of BL-IM system can be analyzed by Interactor algorithm. Here, each output variable y_i ($i = 1, 2, 3$ and 4) would be asked derivative to time gradually, until one or more input variables u_j ($j = 1, 2, 3$ and 4) are obviously included in the derivative functions [22]. The solving steps can be summarized as follows:

$$\dot{y}_1 = x_3 \tag{12}$$
$$\ddot{y}_1 = \frac{K_m}{m} \cdot \frac{L_{m1}}{L_{r1}}[(x_7 + L_{r1l}x_5)u_3 + L_{r1l}x_6u_4] + (k_s x_1 + F_{L\alpha})/m \tag{13}$$
$$\dot{y}_2 = x_4 \tag{14}$$
$$\ddot{y}_2 = \frac{K_m}{m} \cdot \frac{L_{m1}}{L_{r1}}[L_{r1l}x_6u_3 - (x_7 + L_{r1l}x_5)u_4] + (k_s x_2 + F_{L\beta})/m \tag{15}$$
$$\dot{y}_3 = L_{m1}\delta x_5 - \delta x_7 \tag{16}$$
$$\ddot{y}_3 = L_{m1}\delta[-(\gamma - \delta)x_5 + (p_1 x_8 + L_{m1}\delta x_6/x_7)x_6 + \xi\delta\eta x_7 + \xi u_1] - \delta^2(L_{m1}x_5 - x_7) \tag{17}$$
$$\dot{y}_4 = \mu x_6 x_7 - T_L/J \tag{18}$$
$$\ddot{y}_4 = \mu x_7[-(\gamma - \delta)x_6 - (p_1 x_8 + L_{m1}\delta x_6/x_7)x_5 - \xi\eta x_7 p_1 x_8 + \xi u_2] + \mu\delta x_6(L_{m1}x_5 - x_7) \tag{19}$$

Setting:

$$Y = [\ddot{y}_1, \ddot{y}_2, \ddot{y}_3, \ddot{y}_4]^T \tag{20}$$

Combining the selected state variable, the air-gap flux-linkage components ψ_{1d} and ψ_{1q} in (5) can be rewritten as follows:

$$\begin{cases} \psi_{1d} = L_{m1}/L_{r1}(x_7 + L_{r1l}x_5) \\ \psi_{1q} = L_{m1}/L_{r1}L_{r1l}x_6 \end{cases} \tag{21}$$

From (12)∼(19), the Jacobi matrix of the BL-IM system can be derived as follow:

$$A = \frac{\partial Y}{\partial u} = \begin{bmatrix} 0 & 0 & \frac{K_m}{m}\psi_{1d} & \frac{K_m}{m}\psi_{1q} \\ 0 & 0 & \frac{K_m}{m}\psi_{1q} & -\frac{K_m}{m}\psi_{1d} \\ \delta\xi L_{m1} & 0 & 0 & 0 \\ 0 & \mu\xi x_7 & 0 & 0 \end{bmatrix} \tag{22}$$

In the normal operation of BL-IM system, the component of rotor flux-linkage along the d axis and the component of air-gap flux-linkage along the d axis don't equal to zero [22]. Then, $\det(A) \neq 0$, $rank(A) = 4$, the Jacobi matrix is full rank. The relative order of the BL-IM system is: $\alpha = (\alpha_1, \alpha_2, \alpha_3, \alpha_4) = (2, 2, 2, 2)$. The sum of α_i ($i = 1, 2, 3$ and 4) equals to the order of the state equation of the BL-IM system, i.e. $\sum \alpha_i = 8 = n$, then the BL-IM system is reversible [22]. From the implicit function, the inverse system model that takes the current dynamics of torque system into account can be expressed as follow:

$$U = [u_1, u_2, u_3, u_4]^T = \xi^T(\ddot{y}_1, \dot{y}_1, y_1, \ddot{y}_2, \dot{y}_2, y_2, \ddot{y}_3, \dot{y}_3, y_3, \ddot{y}_4, \dot{y}_4, y_4) \tag{23}$$

From (13), (15), (17), (19), it can be known that there is a serious non-linear relationship between the input variable and output variable of BL-IM system, i.e. the inverse system model described by (23) appears serious nonlinearity. In addition, the uncertainty of the BL-IM system, and some other unknown non-linear factors would inevitably affect the decoupling control performance of the analytic inverse system. And then in this paper, in order to overcome the mentioned shortcomings of the analytic inverse system method, utilizing the stronger self-learning and generalization ability of the LS-SVM, the LS-SVM inverse model of a BL-IM system that takes the current dynamics of torque system into account would be identified.

IV. LS-SVM INVERSE SYSTEM DECOUPLING CONTROL STRATEGY OF THE BL-IM SYSTEM

A. REGRESSION PRINCIPLE OF LS-SVM

For training data sets $\{(x_i, y_i)\}_{i=1}^N$, where N is the number of training samples, x_i is the input data, $x_i \in R^n$, y_i is the corresponding output data and $y_i \in R$, utilizing the non-linear mapping relationship $\varphi(\cdot)$, the input space is mapped to a feature space with high dimension. And then the optimal linear regression should be performed. The linear function of the high-dimensional feature space is as follows:

$$y(x) = w^T\varphi(x) + b \tag{24}$$

In (24): w is the weight vector [25], b is the offset value. Defining the "2-norms of error" as the loss function of the LS-SVM, then the optimization problem of the LS-SVM regression algorithms can be expressed as follows:

$$\begin{cases} \min\ J(w, \xi) = \frac{1}{2}w^T w + \gamma\frac{1}{2}\sum_{i=1}^{N}\xi_i^2 \\ s.t.\ y_i = w^T\varphi(x_i) + b + \xi_i,\ i = 1, 2, \ldots, N \end{cases} \tag{25}$$

where: γ is the regularization parameter(or the penalty factor), and it is a compromise parameter between the model generalization ability and the identification accuracy, $\gamma > 0$; ξ is the relaxation factor of the insensitive loss function.

From (25), defining a Lagrange function as follow:

$$L(w, b, \xi, \alpha) = J(w, \xi) - \sum_{i=1}^{N}\alpha_i\left\{w^T\varphi(x_i) + b + \xi_i - y_i\right\} \tag{26}$$

In (26), α_i is the nonnegative Lagrange multiplier.

From the Karush-Kuhn-Tuch (KKT) condition, making the partial derivatives of the Lagrange function to the

parameters w, b, ξ_i and α_i, and taking the obtained partial derivatives as zero [24]. And then:

$$\begin{cases} \dfrac{\partial L}{\partial w} = 0 \rightarrow w = \sum_{i=1}^{N} \alpha_i \varphi(x_i), \\ \dfrac{\partial L}{\partial b} = 0 \rightarrow \sum_{i=1}^{N} \alpha_i = 0, \\ \dfrac{\partial L}{\partial \xi_i} = 0 \rightarrow \alpha_i = \gamma \xi_i, i = 1, 2, \cdots, N \\ \dfrac{\partial L}{\partial \alpha_i} = 0 \rightarrow w^T \varphi(x_i) + b + \xi_i - y_i = 0 \end{cases} \tag{27}$$

After eliminating the parameters w and ξ, following matrix equation can be derived:

$$\begin{bmatrix} 0 & \bar{I}^T \\ \bar{I} & \Omega + \gamma^{-1} I \end{bmatrix} \begin{bmatrix} b \\ \alpha \end{bmatrix} = \begin{bmatrix} 0 \\ y \end{bmatrix} \tag{28}$$

where: $\alpha = [\alpha_1; \cdots; \alpha_N]$, $y = [y_1; \cdots; y_N]$ and $\Omega = \{\Omega_{ij}\}_{N \times N}$ are $N \times N$ dimensional functional matrix; $\Omega_{ij} = \varphi^T(x_i) \cdot \varphi(x_i)$, and $i, j = 1, 2, \ldots, N$; $\bar{I} = [1, 1, \ldots, 1]^T$.

According to the Mercer condition, there exist mapping function $\varphi(\cdot)$ and kernel function $K(\cdot, \cdot)$ that satisfy the condition of "$K(x_i, x_j) = \varphi(x_i)^T \varphi(x_j)$". The commonly used kernel functions include radial basis function, sigmoid function, polynomial function and so on [25]. Because the radial basis function is easy to implement and can obtain better accuracy, then in this paper, the radial basis function as shown in (29) is chosen as the kernel function.

$$K(x_i, x_j) = \exp[-|x_i - x_j|^2 / (2\sigma^2)] \tag{29}$$

where σ is the kernel width.

Calculating the parameters α and b in (28) by the least square method, substituting (27), (29) into (24), then the regression function of the LS-SVM can be derived as follow:

$$y(x) = \sum_{i=1}^{N} \alpha_i K(x_i, x) + b \tag{30}$$

Figure 2 gives the LS-SVM topology that takes the d-axis voltage component u_{s1d} of torque windings as the output variable [22]. The LS-SVM topology that takes other variable as the output variable is similar with this, and no further details will be given here.

B. LS-SVM INVERSE SYSTEM DECOUPLING CONTROL

In this paper, the inverse model of a BL-IM system is realized by way of the LS-SVM and some additional integrators. The schematic diagram of the composite system is shown in Figure 3, which is composed of the trained LS-SVM inverse system and the original BL-IM system. Because a LS-SVM can only be used to approximate a "single output function", then aiming at each output variable, the corresponding LS-SVM inverse model should be constructed firstly. After that, the LS-SVM inverse system should be connected in series before the original BL-IM system, as shown in Figure 3, then the BL-IM system would be decoupled into

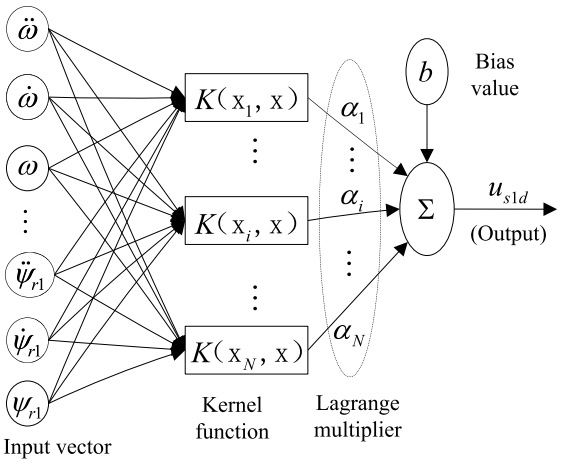

FIGURE 2. Topology of LS-SVM.

four independent second-order pseudo-linear subsystems. At the end, adopting the linear system synthesis method, the controllers for each subsystem can be designed separately, and the dynamic decoupling control among the motor speed, the rotor flux-linkage and the two radial displacement components can be realized. The specific implementation steps can be summarized as follows:

1) ACQUISITION OF TRAINING SAMPLE

In this paper, the training sample set is obtained in the precise analytic inverse control system of a four-pole BL-IM. Taking the random signal with normal distribution in the range of 0.45Wb $\sim$ 0.9Wb as the given rotor flux-linkage, taking the random signal with normal distribution in the range of 0 $\sim$ 3000 r/min as the given speed, and taking the random signal with normal distribution in the range of $-$0.1mm $\sim$ 0.1mm as the given radial displacement component. The whole excitation time is 3.0 seconds, and the sampling step size is set as 0.001 seconds.

The sampled data includes ψ_{r1}, ω_r, α, β, u_{s1d}, u_{s1d}, i_{s2d} and i_{s2q}. After the sampled data are smoothed and filtered, adopting the "high precision five-point numerical differential algorithm", the first and second derivatives of the radial displacement components, rotor flux- linkage and motor speed are obtained. And then, the training sample set of the LS-SVM, i.e. $\{\ddot{\alpha}, \dot{\alpha}, \alpha, \ddot{\beta}, \dot{\beta}, \beta, \ddot{\psi}_{r1}, \dot{\psi}_{r1}, \psi_{r1}, \ddot{\omega}_r, \dot{\omega}_r, \omega_r\}$ and $\{i_{s2d}, i_{s2q}, u_{s1d}, u_{s1q}\}$ are constructed. From the obtained data, selecting 2000 groups at equal intervals as the training set, and the rest data are used as the test set.

2) TRAINING LS-SVM INVERSE SYSTEM MODEL

After the training sample set is determined, taking the $u = \{\ddot{\alpha}, \dot{\alpha}, \alpha, \ddot{\beta}, \dot{\beta}, \beta, \ddot{\psi}_{r1}, \dot{\psi}_{r1}, \psi_{r1}, \ddot{\omega}_r, \dot{\omega}_r, \omega_r\}$ as the training inputs, using i_{s2d}, i_{s2q}, u_{s1d} and u_{s1q} as the training outputs. Aiming at each of the training output variable, the off-line training of LS-SVM inverse model is made. There are four learning machines that are established to train the LS-SVM. In the training process of LS-SVM,

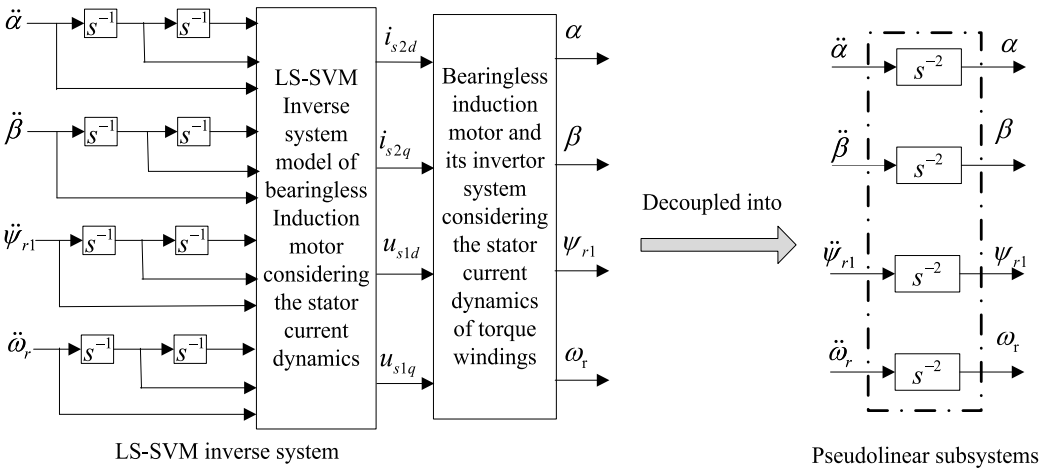

FIGURE 3. LS-SVM inverse system decoupling Schematic diagram of a BL-IM.

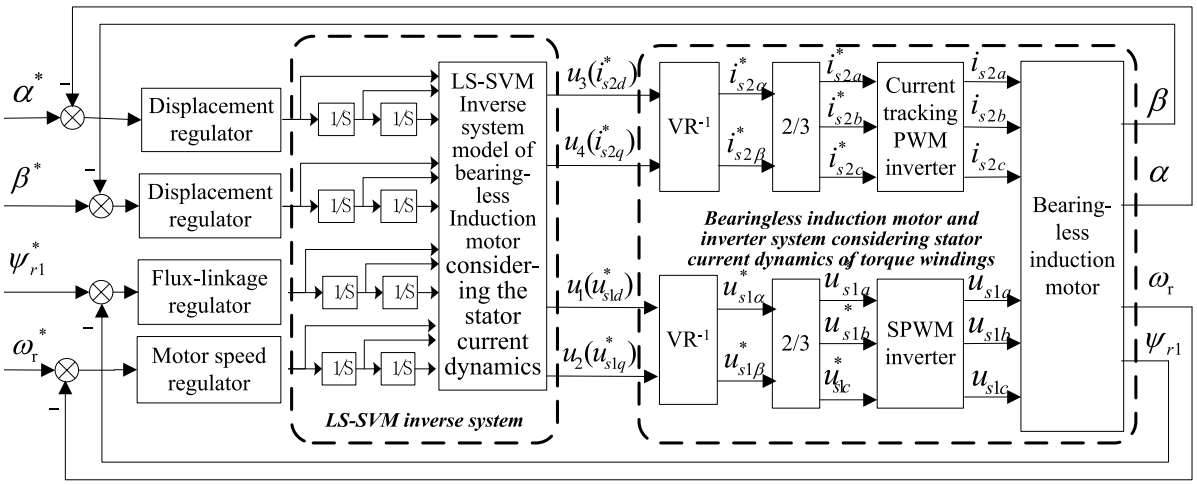

FIGURE 4. Considering the current dynamics of torque windings, the trained LS-SVM inverse model is corrected in front of original BL-IM system, the BL-IM system is decoupled into four second-order subsystems, the PD regulator with a first-order inertia link is used as the regulator of each subsystem, then the LS-SVM inverse decoupling control system a BL-IM is constructed.

the regularization parameter γ, and the kernel width parameter σ of the radial basis function determine the training accuracy and complexity of the LS-SVM [25]. Here, the grid search method is used to obtain the best regularization parameter and the kernel width [25], and then the LS-SVM inverse model with a higher training accuracy is obtained.

3) CONTROL SYSTEM SYNTHESIS

After the off-line trained LS-SVM inverse system is combined with the original BL-IM system, the BL-IM system is decoupled into four pseudo-linear second-order integral subsystems, include a motor speed subsystem, a rotor flux-linkage subsystem and two radial displacement component subsystems [22]. In order to obtain excellent static- and dynamic-characteristics, and improve the anti-interference ability, a closed-loop regulator is added to each subsystem. Then the linearized decoupling controller of the BL-IM system is composed of the closed-loop regulators and the LS-SVM inverse system obtained by training. Here, the PD regulator with a first-order inertia link is used as the closed-loop regulator of each subsystem, its transfer function is "$G(s) = K(\tau_1 s + 1)/(\tau_2 s + 1)$", where the τ_1 and τ_2 are the differential- and inertial-time constants respectively. Then the decoupled subsystem is corrected as a "Typical-II" subsystem, its open loop transfer function is as follow:

$$G_{ol}(s) = \frac{K(\tau_1 s + 1)}{s^2(\tau_2 s + 1)} \tag{31}$$

Figure 4 shows the LS-SVM inverse decoupling control system block diagram of a BL-IM. Compared with the existing LS-SVM inverse decupling control system [28], [29], the advantage is that in the identified LS-SVM inverse system model, because the stator current dynamics of the torque system has been taken into account, the closed-loop current regulator of the torque windings can be omitted naturally,

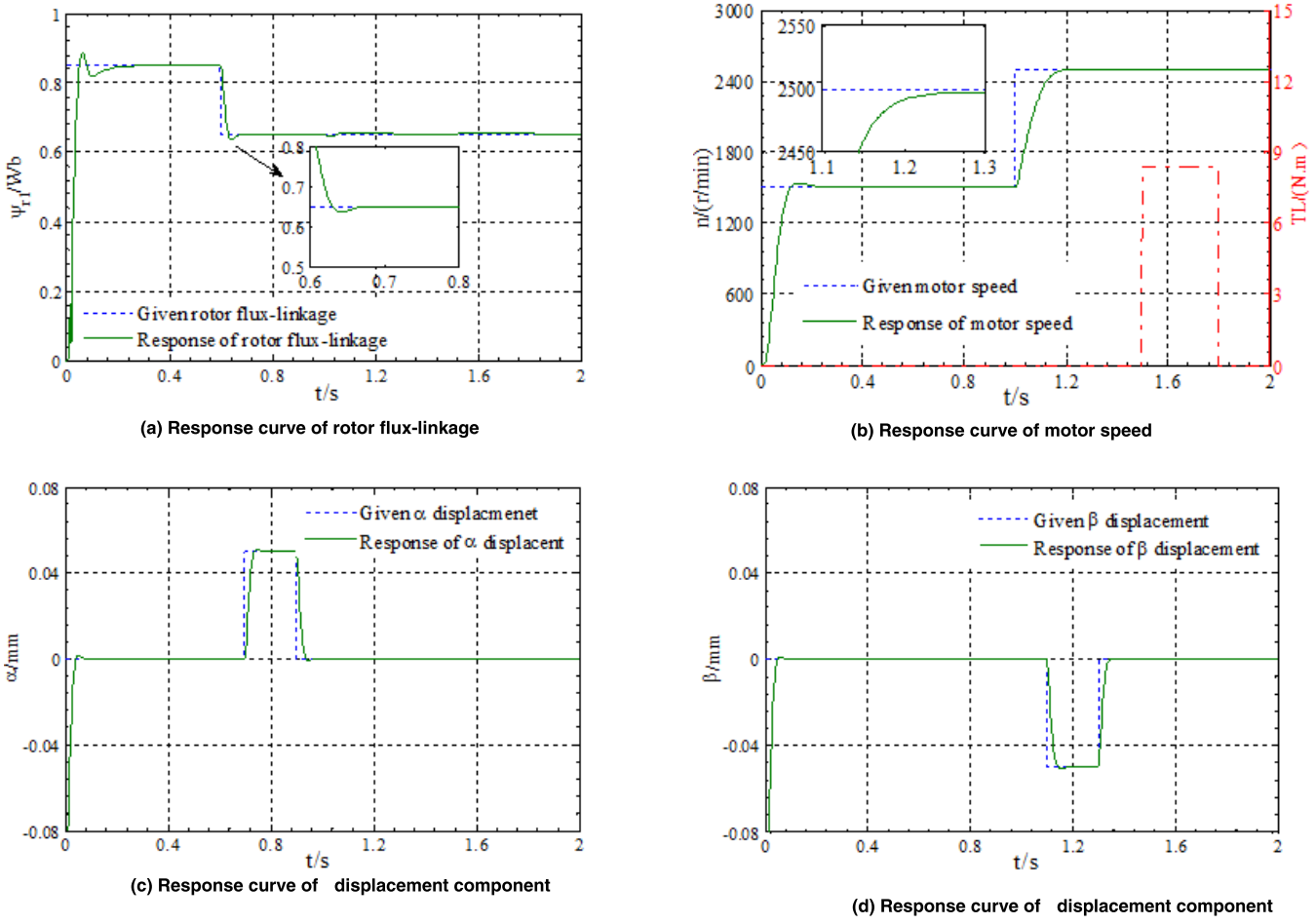

(a) Response curve of rotor flux-linkage

(b) Response curve of motor speed

(c) Response curve of displacement component

(d) Response curve of displacement component

FIGURE 5. Response curves of LS-SVM inverse decoupling control system.

and then the overall control system structure of the BL-IM could be simplified to a certain extent.

V. SYSTEM SIMULATION VERIFICATION AND ANALYSIS

According to the control system structure shown in Figure 4, the system simulation analysis and verification are carried out, Table 1 presents the specific parameters of a BL-IM.

Simulation conditions: setting the initial radial displacement components $\alpha_0 = -0.1$mm, $\beta_0 = -0.12$mm; the given rotor flux-linkage $\psi^* = 0.85Wb$, the given motor speed $n^* = 1500r/min$, the given radial displacement components α^* and β^* equal to zero; the system starts with no load.

Figure 5 shows the response waveforms of the proposed LS-SVM inverse decoupling control system. In order to facilitate the comparative analysis, under the same simulation conditions, the comparative response waveforms of the analytic inverse decoupling control system are given in Figure 6.

From the Figure 5 and Figure 6, the specific comparative results can be summarized as follows:

1) In the no-load start-up process: based on the proposed LS-SVM inverse decoupling control method, the motor speed overshoot is only about 2%, the α- and β-displacement components can reach their given values quickly with almost no overshoots, the overshoot of rotor flux-linkage is about 4.7%; but when the analytical inverse decoupling control

TABLE 1. Parameters of a BL-IM.

Parameters	Description	Value
r	Inner diameter of stator (mm)	62
l	effective core length (mm)	82
δ_l	Air-gap of the auxiliary bearing (mm)	0.2
P	Power of the motor (kW)	2.2
R_s	Resistance of the torque windings (Ω)	1.6
R_r	Resistance of the rotor windings (Ω)	1.423
L_{sl1}	leakage inductance of the torque windings (H)	0.0043
L_{rl1}	Leakage-inductance of the rotor windings (H)	0.0043
L_{m1}	mutual inductance of the torque system (H)	0.0859
J	rotation inertia (kg.m^2)	0.024
R_{s2}	Resistance of the suspension windings	2.7
L_{s2l}	leakage inductance of suspension windings (H)	0.00398
L_{m2}	mutual inductance of the suspension system (H)	0.230

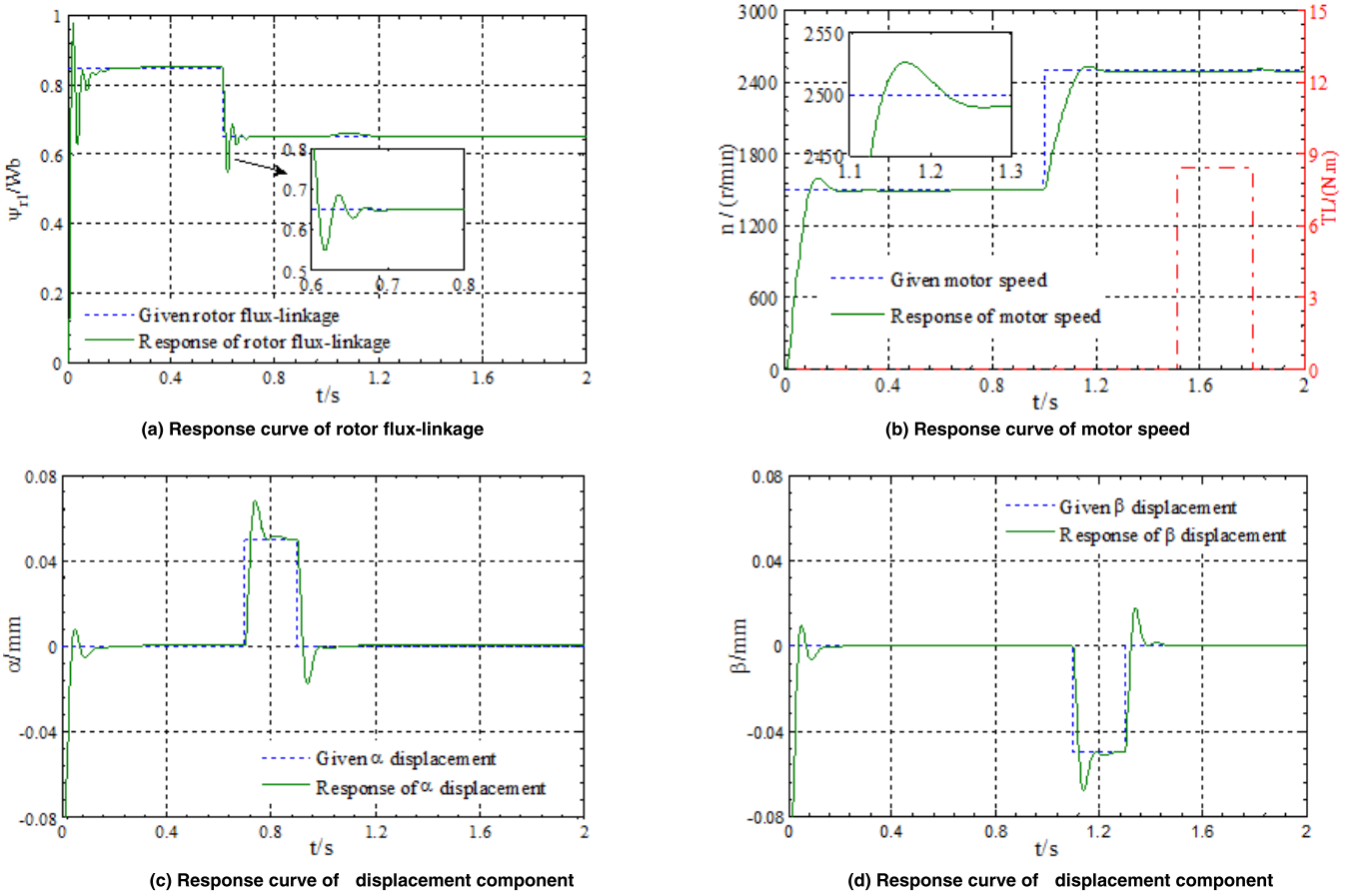

(a) Response curve of rotor flux-linkage

(b) Response curve of motor speed

(c) Response curve of displacement component

(d) Response curve of displacement component

FIGURE 6. Response curves of analytical inverse decoupling control system.

method is adopted, the motor speed overshoot is about 6%, the overshoot of flux-linkage is about 20%, the overshoots of the α- and β-displacement components are about 0.01mm. The simulation results have shown that when the proposed LS-SVM inverse decoupling control method is adopted, a better starting performance can be achieved.

2) In order to verify the decoupling performance of the proposed LS-SVM inverse system method, the given signal of each controlled variable is changed at different time. At 0.6s, the given signal of rotor flux-linkage is suddenly changed to 0.65Wb; the given signal of the radial displacement in α direction is suddenly changed to 0.05mm at 0.7s, and restored to zero at 0.9s; the given signal of motor speed is suddenly changed to 2500r/min at 1.0s; the given signal of the radial displacement in β direction is suddenly changed to -0.05 mm at 1.1s, and restored to zero at 1.3s.

From Figure 5, it can be seen that when one controlled variable changes, the other controlled variables don't change significantly. The simulation results have shown that the LS-SVM inverse system method can realize the dynamic decoupling control among the rotor flux-linkage, motor speed and two radial displacement components.

Comparing Figure 5 with Figure 6, it can be seen that for the LS-SVM inverse decoupling control system, during the transition process of variable mutation, the overshoot of the rotor flux-linkage is no more than 0.04Wb, as for the motor speed, α- and β-displacement components, there are almost no overshoots. while for the analytical inverse decoupling control system, during the transition process of variable mutation, the overshoot of the rotor flux-linkage is about 0.1Wb, the overshoot of the motor speed is about 50r/min, the overshoots of α- and β-displacement components are about 0.01mm. The simulation results have shown that comparing with the analytical inverse decoupling control system, during the transition process of variable mutation, the LS-SVM inverse decoupling control system has smaller overshoot and shorter adjustment time, and then it has better tracking control performance.

3) In order to verify the anti-disturbance ability, the load torque of 8.4N.m is suddenly added at 1.5s. Comparing Figure 5(b) with Figure 6(b), it can be seen that for the LS-SVM inverse decoupling control system, the motor speed decreases by only about 0.5% under the sudden load, and it can be restored to the set value in a very short time; while for the analytical inverse decoupling system, the motor speed decreases by about 1.0%. The simulation results have shown that based on the LS-SVM inverse system decoupling control method, the BL-IM system owns stronger robustness and stronger anti-disturbance ability. In addition, in the process of sudden loading and unloading, the two radial displacement

components in Figure 5(c) and Figure 5(d) are almost unaffected or very little affected, the good dynamic decoupling control performance between torque system and suspension system is verified again.

VI. CONCLUSION

The bearingless induction motor (BL-IM) is a nonlinear, multivariable and strongly coupled object. In order to improve its dynamic control performance, under the conditions of considering the dynamic characteristics of the stator current of torque system, an inverse system decoupling control strategy based on LS-SVM is proposed, and the system simulation and verification analysis are carried out. The specific research conclusions are summarized as follows:

1) After considering the stator current dynamics of torque system, the BL-IM system oriented by the rotor flux-linkage, is an eight-order nonlinear and strongly coupled complex system that has four input variables and four output variables, the BL-IM system is reversible. In addition, since the components of stator voltage are selected as the input variables of the original torque system, the current closed-loop of the torque windings can be eliminated, and the overall control system structure of the BL-IM can be effectively simplified.
2) Based on the approximation and identification fitting ability of the LS-SVM, the inverse system model can be obtained by off-line learning, and then the dependence of the traditional analytical inverse system method on the accurate model of the BL-IM system can be effectively overcome.
3) Adopting the proposed LS-SVM inverse system decoupling control method, the dynamic decoupling control between the motor speed, rotor flux-linkage and two radial displacement components can be realized. Comparing with the traditional analytical inverse system of BL-IM, the proposed LS-SVM inverse decoupling control system of BL-IM has many advantages, such as smaller overshoot, better tracking performance and stronger robustness.

REFERENCES

[1] X. Yao and Z. B. Chen, "Sliding mode control with deep learning method for rotor trajectory control of active magnetic bearing system," *Trans. Inst. Meas. Control*, vol. 41, no. 5, pp. 1383–1394, Mar. 2019.
[2] X. Cheng, B. Wang, Q. Chen, L. Zhang, H. Liu, and S. Song, "A unified design and the current ripple characteristic analysis of digital switching power amplifier in active magnetic-levitated bearings," *Int. J. Appl. Electromagn. Mech.*, vol. 55, nol.3, pp. 391–407, Jan. 2017.
[3] M. Komori, K. Yamanaka, K. Asami, and N. Sakai, "Proposal of new superconducting magnetic bearing using high $T_c$superconducting bulk and coil," *IEEE Trans. Magn.*, vol. 54, no. 11, Nov. 2018, Art. no. 8300304. doi: 10.1109/TMAG.2018.2841943.
[4] C. Dumont, V. Kluyskens, and B. Dehez, "Linear state-space representation of heteropolar electrodynamic bearings with radial magnetic field," *IEEE Trans. Magn.*, vol. 52, no. 1, Jan. 2016, Art. no. 8100109. doi: 10.1109/TMAG.2015.2475239.
[5] W. Bu, X. Zhang, Y. Qiao, Z. Li, and H. Zhang, "Equivalent two-phase mutual inductance model and measurement algorithm of three-phase bearingless motor," *Trans. Inst. Meas. Control*, vol. 40, no. 2, pp. 630–639, Jan. 2018.
[6] X. Sun, B. Su, L. Chen, Z. Yang, J. Chen, and W. Zhang, "Nonlinear flux linkage modeling of a bearingless permanent magnet synchronous motor based on AW-LSSVM regression algorithm," *Int. J. Appl. Electromagn. Mech.*, vol. 51, pp. 151–159, Jun. 2016.
[7] W.-S. Bu, C.-L. Zu, and C.-X. Lu, "Inverse system analysis and modeling of bearingless induction motor and its combined control strategy," *Math. Problems Eng.*, vol. 2014, Jun. 2014, Art. no. 698171.
[8] W. Bu, B. Li, and C. Lu, "Decoupling control strategy of BLIM considering rotor mass eccentricity," *J. Control Sci. Eng.*, vol. 2018, Oct. 2018, Art. no. 9579125.
[9] Z. Yang, X. Chen, X. Sun, C. Bao, and J. Lu, "Rotor radial disturbance control for a bearingless induction motor based on improved active disturbance rejection control," *Int. J. Comput. Math. Elect. Electron. Eng.*, vol. 38, no. 1, pp. 138–152, Jan. 2019.
[10] W. Bu, Y. Chen, and C. Zu, "Stator flux orientation inverse system decoupling control strategy of bearingless induction motor considering stator current dynamics," *IEEJ Trans. Elect. Electron. Eng.*, vol. 14, no. 4, pp. 640–647, Apr. 2019.
[11] Y. Sun, B. Su, and X. Sun, "Optimal design and performance analysis for interior composite-rotor bearingless permanent magnet synchronous motors," *IEEE Access*, vol. 7, pp. 7456–7465, 2019.
[12] Z. Hao, H. Zhu, Y. Cheng, and L. Huang, "Speed control of bearingless permanent magnet synchronous motor based on flux strengthening and voltage regulation," *IEEE Access*, vol. 6, pp. 72392–72401, 2018. doi: 10.1109/ACCESS.2018.2880276.
[13] X. Sun, Z. Xue, J. Zhu, Y. Guo, Z. Yang, L. Chen, J. Chen, "Suspension force modeling for a bearingless permanent magnet synchronous motor using maxwell stress tensor method," *IEEE Trans. Appl. Supercond.*, vol. 26, no. 7, Oct. 2016, Art. no. 0608705. doi: 10.1109/TASC.2016.2599708.
[14] Z. Yang, D. Zhang, X. Sun, and X. Ye, "Adaptive exponential sliding mode control for a bearingless induction motor based on a disturbance observer," *IEEE Access*, vol. 6, pp. 35425–35434, 2018.
[15] H. Zhu and F. Li, "Optimization design of bearingless permanent-magnet slice motor," *IEEE Trans. Appl. Supercond.*, vol. 26, no. 4, Jun. 2016, Art. no. 5202804. doi: 10.1109/TASC.2016.2516915.
[16] H. Jia, J. Wang, M. Cheng, W. Hua, and S. Fei, "Mathematical model of radial suspending force for a new stator-permanent magnet bearingless machine," *IEEE Trans. Magn.*, vol. 51, no. 11, Nov. 2015, Art. no. 8205104. doi: 10.1109/TMAG.2015.2439960.
[17] X. Sun, L. Chen, H. Jiang, Z. Yang, J. Chen, and W. Zhang, "High-performance control for a bearingless permanent-magnet synchronous motor using neural network inverse scheme plus internal model controllers," *IEEE Trans. Ind. Electron.*, vol. 63, no. 6, pp. 3479–3488, Jun. 2016.
[18] W. Bu, X. Zhang, and F. He, "Sliding mode variable structure control strategy of bearingless induction motor based on inverse system decoupling," *IEEJ Trans. Electr. Electron. Eng.*, vol. 13, pp. 1052–1059, Jul. 2018.
[19] X. Ye, Z. Yang, and T. Zhang, "Modelling and performance analysis on a bearingless fixed-pole rotor induction motor," *IET Electr. Power Appl.*, vol. 13, no. 2, pp. 251–258, Feb. 2019.
[20] Z. Yang, K. Wang, X. Sun, and X. Ye, "Load disturbance rejection control of a bearingless induction motor based on fractional-order integral sliding mode," *Proc. Inst. Mech. Eng. I, J. Syst. Control Eng.*, vol. 232, no. 10, pp. 1356–1364, Nov. 2018.
[21] Z.-Q. Wang and X.-X. Liu, "Nonlinear internal model control for bearingless induction motor based on neural network inversion," *Acta Automatica Sinica*, vol. 39, no. 4, pp. 433–439, Apr. 2013.
[22] W. Bu, F. He, Z. Y. Li, H. Zhang, and J. Shi, "Neural network inverse system decoupling control strategy of BLIM considering stator current dynamics," *Trans. Inst. Meas. Control*, vol. 41, no. 3, pp. 621–630, Feb. 2019.
[23] W. Bu, Y. Huang, C. Lu, H. Zhang, and H. Shi, "Unbalanced displacement LMS extraction algorithm and vibration control of a bearingless induction motor," *Int. J. Appl. Electromagn. Mech.*, vol. 56, no. 1, pp. 35–47, 2018.
[24] W. Bu, B. Li, F. He, and J. W. Li, "Inverse system decoupling sliding mode control strategy of BLIM considering current dynamics," *Int. J. Appl. Electromagn. Mech.*, vol. 60, no. 3, pp. 1–16, Dec. 2018.
[25] W. Bu, Z. Li, and C. Lu, X. Wang, and J. Xiao, "Research on the least squares support vector machine displacement observer of a bearingless induction motor," *Trans. Inst. Meas. Control*, vol. 39, no. 5, pp. 688–697, May 2017.

[26] V. N. Vapnik, "An overview of statistical learning theory," *IEEE Trans Neural Netw.*, vol. 10, no. 5, pp. 988–999, Sep. 1999.
[27] J. A. K. Suykens, J. Vandewalle, and B. De Moor, "Optimal control by least squares support vector machines," *Neural Netw.*, vol. 14, no. 1, pp. 23–25, Jan. 2001.
[28] K. Li, G. Cheng, X. Sun, and Z. Yang, "A nonlinear flux linkage model for bearingless induction motor based on GWO-LSSVM," *IEEE Access*, vol. 7, pp. 36558–36567, 2019.
[29] W. Zhengqi and H. Xueliang, "Nonlinear decoupling control for bearingless induction motor based on support vector machines inversion," (in Chinese), *Trans. China Electrotech. Soc.*, vol. 30, no. 10, pp. 164–170, Oct. 2015.
[30] Z. Yang, X. Sun, X. Zhang and H. Zhu, "Decoupling control of bearingless induction motors based on least squares support vector machine inverse," *J. Comput. Theor. Nanosci.*, vol. 11, no. 5, pp. 1403–1409, May 2014.
[31] L. Wan, Z. Yang, X. Sun, Z. Chen, and L. Chen, "Decoupling control of a 5-degree-of-freedom bearingless induction motor based on least squares support vector machine inverse," *Adv. Mech. Eng.*, vol. 8, no. 10, pp. 1–11, Oct. 2016. doi: 10.1177/1687814016672120.

WENSHAO BU was born in Luohe, China, in 1969. He received the B.S. degree in electrical engineering from the Hefei University of Technology, Hefei, China, in 1993, the M.S. degree in macaronis engineering from the Henan University of Science and Technology, Luoyang, China, in 2001, and the Ph.D. degree in electrical engineering from the Huazhong University of Science and Technology, Wuhan, China, in 2007.

In 1993, he joined Luoyang Bearing Group Corporation, as an Engineer. In 2001, he joined as a Senior Lecturer at the Henan University of Science and Technology, where he has been a Professor, since 2014. His research interests include new type electrical machine and its control systems, power electronics, and controlling theory and its application.

ZIYUAN LI was born in Shangqiu, China, in 1989. He received the B.S. degree in electrical engineering from the Henan University of Science and Technology, Luoyang, China, in 2013, where he is currently pursuing the master's degree. His research interest includes bearingless motor and its control technology.